SPECTROSCOPY
OF CONDENSED MATTER

Solvatochromic Study of Supramolecular Amphiphile Based on Calix[4]arene Connected to a Fluorescent Benzofurazan Moiety at Lower Rim: Evaluation of Ground and Excited State Dipole Moments

S. Joshi*

Amity School of Applied Sciences, Department of Physics, Amity University, Rajasthan, Jaipur, India
*e-mail: sunita.joshi.2006@gmail.com

Abstract—Photophysical properties of a supramolecular amphiphile of calix[4]arene having benzofurazan moiety at the lower rim, **L**, has been studied. Electronic absorption and fluorescence spectra of **L** have been recorded in wide range of solvents of different polarities and data were used to study solvatochromic properties. The ground state and the excited state dipole moment of **L** were estimated from the Bakhshiev's and Bilot-Kawaski's equations. High value of dipole moment is observed for excited state as compared to ground state value and this is attributed to more polar excited state of molecule. Also, fluorescence emission peak undergoes a bathochromic shift with increase in the polarity of the solvent, confirming $\pi \to \pi^*$ transition. Scanning electron microscopy reveals that the aggregation of **L** is increased on going from the polar to non polar solvents.

INTRODUCTION

Investigating photophysical properties of fluorescent probes has been a subject of interest for many researchers due to their potential applications as sensors, optoelectronics, and in biomedical field. Photophysical studies of the molecules, especially estimation of ground and excited state dipole moments and the effect of solvent polarity on the fluorophore remains an area of great interest [1–7]. Such studies received tremendous progress due to their wide utility in a variety of applications that can be extended to different fields. A number of techniques such as electronic polarization of fluorescence, electric–dichroism, microwave conductivity and stark splitting are useful in the determination of excited-state dipole moment [2, 8], but due to the drawbacks such as equipment sensitivity and being focussed only to study simple molecules, the application of these is limited. The solvatochromic method is one of the simpler ones, which is based on the shift of absorption and or fluorescence maxima in different solvents of varying polarity and this is being used to determine the dipole moments of different molecules [9, 10]. However, the thrust is more so particularly in case of complex molecular frameworks with fluorophores. Benzooxadiazole is a fluorescent molecule and its derivatives have been studied for their photophysical properties

[11–14]. In spite of considerable number of literature reports, many of the photophysical characteristics of the benzooxadiazole are under exploration and their solvatochromic properties are of great interest if such moieties are attached to supramolecular platforms, such as, those of calix[n]arenes. Indeed the derivatization of calix[4]arene platform has proven well as ion and molecular receptors, as biosensors, as catalysts, as biomimetic models, and as templates for forming supramolecular aggregates [15–21]. As the solvatochromic and photo-physical studies of the calix[4]arene-conjugates is under explored, such studies pertinent to this kind of supramolecular and amphiphile molecular system would enrich the relevant area.

Therefore, we report the solvatochromic and photo-physical properties of a calix[4]arene framework that is functionalized with benzooxadiazole to result in a lower rim 1,3-di-conjugate of calix[4]arene (**L**). Herein, we also studied the ground and excited state dipole moments of the calix[4]arene conjugate **L** using Bakshiev's and Bilot–Kawski's equations [22–24] which are dependent on solvatochromic shift method, their fluorescence decay life times were measured by time correlated single photon counting (TCSPC) method, demonstrated its potential as sensitive fluorophore for the varying polarity range of the

solvents. Further, the supramolecular features of **L** in various solvents have been explored by microscopy methods.

EXPERIMENTAL

All the solvents used for the spectroscopy studies were of AR grade and were distilled and dried immediately before use. The absorption studies were carried out on Cary 100 Bio UV–visible spectrophotometer and the fluorescence studies on a Varian–Cary eclipse fluorescence spectrophotometer. The stock solutions of **L** were prepared in different solvents and then further diluted to give a final cuvette concentration of **L** as 20 μM in all the cases. Excitation and emission slit widths used were 2.5 nm and a scan speed of 200 nm/min was used. The fluorescence lifetimes were measured from time resolved intensity decays by the method of time correlated single photon counting (TCSPC) technique. The light source used was picoseconds diode laser (Nano LED) at 440 nm (Horiba JobinYvon, USA). The fluorescence decays were deconvoluted using the data station software for acquisition and IBH DAS6 for data analysis. The signals were collected at the magic angle of 54.7°. The decay times were determined using non-linear least square method of TCSPC technique. Goodness of the fits was evaluated by the χ^2 criterion and the randomness of the residuals of the fitted function to data. Care was taken in data analysis to differentiate between the mono-, bi-, and tri-exponential fits by judging the χ^2 values, standard deviation and weighted residuals. For all the lifetime measurements, fluorescence decays were analyzed by multi-exponential iterative fitting program provided by DAS-6 decay analysis software:

$$I(t) = \sum_i \alpha_i \exp(t/\tau_i),$$

where α_i is a pre-exponential factor representing the fractional contribution to the time resolved decay of the component with a lifetime τ_i. The average fluorescence lifetimes were calculated using the relation

$$\langle \overline{\tau} \rangle = \frac{\sum_i \alpha_i \tau_i^2}{\sum_i \alpha_i \tau_i}.$$

Quantum Yield Calculation

The fluorescence quantum yield was determined by using quinine sulphate in 0.1 M sulfuric acid ($\Phi = 0.54$) as the reference [25]. The quantum yield is calculated using the equation [26]

$$\phi_s = \phi_r \frac{F_s A_r \eta_s^2}{F_r A_s \eta_r^2},$$

where the subscript r and s refers to the reference and sample, respectively. The A, F, and η refers to the absorbance, fluorescence intensity and the refractive index, respectively, in the corresponding solvent.

Sample Preparation for Microscopy

All the samples for scanning electron microscopy (SEM) were prepared at 6×10^{-4} M in different solvents and the solutions were sonicated for 10 min before these were drop casted on aluminium foil and allowed to dry under IR lamp.

Synthesis and Characterization of *L*

As the synthesis of *p-tert*-butyl calix[4]arene, its lower rim 1,3-bis-propyl-phthalimide derivative and its 1,3-bis-propylamine derivative were already known [27], the synthesis of the last step to give **L** and its characterization are given. To a solution of 7-chloro-4-nitro benzooxadiazole (0.438 g, 2.2 mmol) in dry ethanol, P_2 was added (0.95 g, 1.24 mmol) along with a catalytic amount of dry pyridine. The reaction was stirred at room temperature for one day. The solvent was removed under reduced pressure and the residue was purified by silica gel column chromatography using ethyl acetate: pet ether in 20 : 80 as eluting medium. Orange solid; yield (0.96 g, 70%); melting point 224−226°C; ^{1}H-NMR (400 MHz, DMSO-d$_6$) δ 8.50 (s, 2H, −NH), 8.34 (d, 2H, −ArH), 7.15 (s, 4H, −ArH), 7.13 (s, 4H, −ArH), 6.37 (d, 2H, −ArH), 4.20 (d, 4H, −CH$_2$Ar), 4.061 (t, 4H, −OCH$_2$), 3.83 (t, 4H, −NCH$_2$), 3.43(d, 4H, −CH$_2$Ar), 2.38 (m, 4H, −CH$_2$−), 1.18 (s, 18H, −tCH$_3$), 1.10 (s, 18H, −tCH$_3$). ^{13}C-NMR: 150.5, 150.1, 147.7, 145.1, 144.4, 144.2, 142.0, 137.8, 133.5, 127.9, 126.2, 125.8, 121.6, 99.4, 74.3, 41.1, 34.5, 31.8, 31.3, 29.5, 29.7. ^{13}C-NMR (^{135}DEPT): 137.8, 126.2, 125.8, 99.4, 74.3, 41.1, 31.8, 31.3, 29.5, 28.7. HRMS (ESI-TOF) *m/z*: [M + Na]$^+$. Calcd. for $C_{62}H_{72}N_8NaO_{10}$ 1111.526; found 1111.555.

RESULTS AND DISCUSSION

Synthesis and Characterization of *L*

The **L**, whose structure is given in Scheme 1, was synthesized in three steps starting from *p-tert*-butyl-calix[4]arene (C4A) and then by going through its lower rim 1,3-bis-propyl-phthalimide derivative and its 1,3-bis-propylamine derivative and then the **L** as given in Scheme 1. The ^{1}H NMR spectrum of **L** exhibits cone conformation as judged based on the bridge −CH$_2$ peak pattern that shows two doublets (3.4 and 4.2 ppm) characteristic of the cone conformation the calix[4]arene platform.
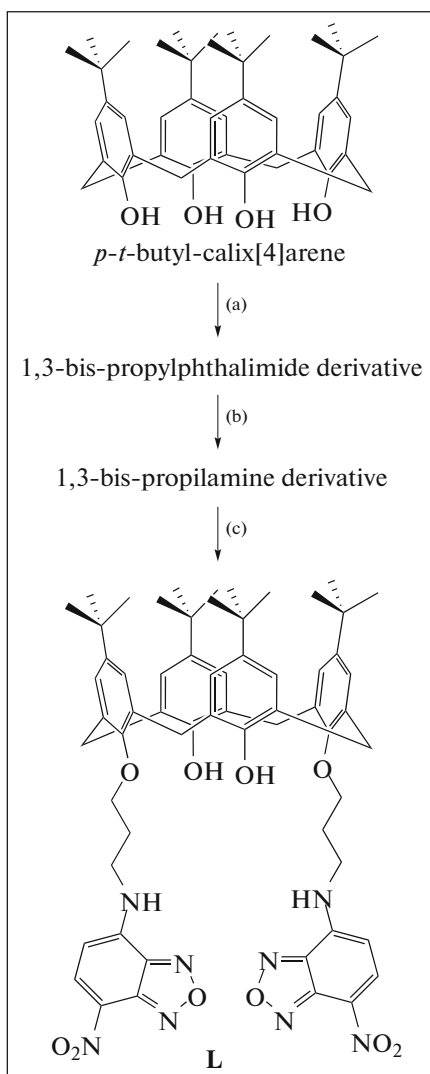
Scheme 1. Synthesis of **L**. (a) 3-Bromopropyl pthalimide, K_2CO_3, acetonitrile, 24 h at reflux; (b) hydrazine hydrate, C_2H_5OH, 12 h at reflux; (c) 7-chloro 4-nitro benzooxadi-azole, dry pyridine, EtOH, rt for 24 h.

Effect of Solvent on Absorption and Emission Spectra of L

Absorption and fluorescence spectra of **L** were measured in different solvents of varying polarity. The photophysical properties of **L** are solvent dependent owing to its donor-acceptor property as well as its amphiphilic property. The absorption spectra of **L** in different solvents of varying polarity are given in Fig. 1a and the corresponding spectral data are reported in Table 1. The absorption of **L** is character-ized by $\pi \to \pi^*$ transition from benzofurazan moiety whose λ_{max} is in the range 454 to 465 nm depending upon the solvent and exhibits a fairly linear trend with respect to the polarity of the medium as given in Fig. 1b. With increase in the polarity of the medium, ~10 nm red shift was observed in the absorption band suggesting that the ground state of the molecule is polar. The extinction coefficient values have been derived in case of four different solvents (in a range from nonpolar to polar) and high values of extinction coefficient were observed, suggesting that the elec-tronic transition from the ground state to the excited state has $\pi \to \pi^*$ character (Fig. 2).

The fluorescence emission spectra of **L** in different solvents are given in Fig. 1d and the spectra showed substantial red shift of ~42 nm in λ_{em}^{max} on going from highly non-polar CCl_4 to highly polar DMSO and the corresponding linear plot given in Fig. 1e and this is attributable to the orientation of solvent dipoles w.r.t. the fluorophore. However, we observed larger shift in emission spectra compared to the absorption spectra. Thus, the **L** is more polar in the excited state as com-pared to the ground state. The fluorescence quantum yield (Φ) of the receptor **L** increases as the relative polarity parameter increases up to a value of ~0.2 and remains unaltered thereafter, with the exception being noticed in case of THF and acetonitrile where in greater Φ values were observed (Fig. 1f). Thus, the Φ for **L** varies from 30 to 69% depending on the polarity and hydrogen bonding ability of the solvent (Table 1).

### Solvent Dependent Morphology of L

The **L** showed shifts in the absorption and fluores-cence spectra by varying the solvent indicating that the nature of the interaction of **L** varies by varying the sol-vent polarity. The affect of this has been examined based on their surface structures using scanning elec-tron microscopy (SEM) (Fig. 3), since the conjugates

**Table 1.** Spectroscopic data of **L** in different solvents

| Solvent	λ_{abs}^{max}, nm	λ_{em}^{max}, nm	Φ	Solvent	λ_{abs}^{max}, nm	λ_{em}^{max}, nm	Φ
DMSO	465	541	0.39	THF	459	520	0.69
DMF	463	532	0.42	Chloroform	458	516	0.46
Acetonitrile	461	526	0.55	DEE	456	515	0.45
Methanol	462	530	0.38	Toulene	455	511	0.42
Isopropanol	462	528	0.40	CCl_4	453	499	0.36
DCM	460	522	0.42	*n*-Hexane	454	500	0.30
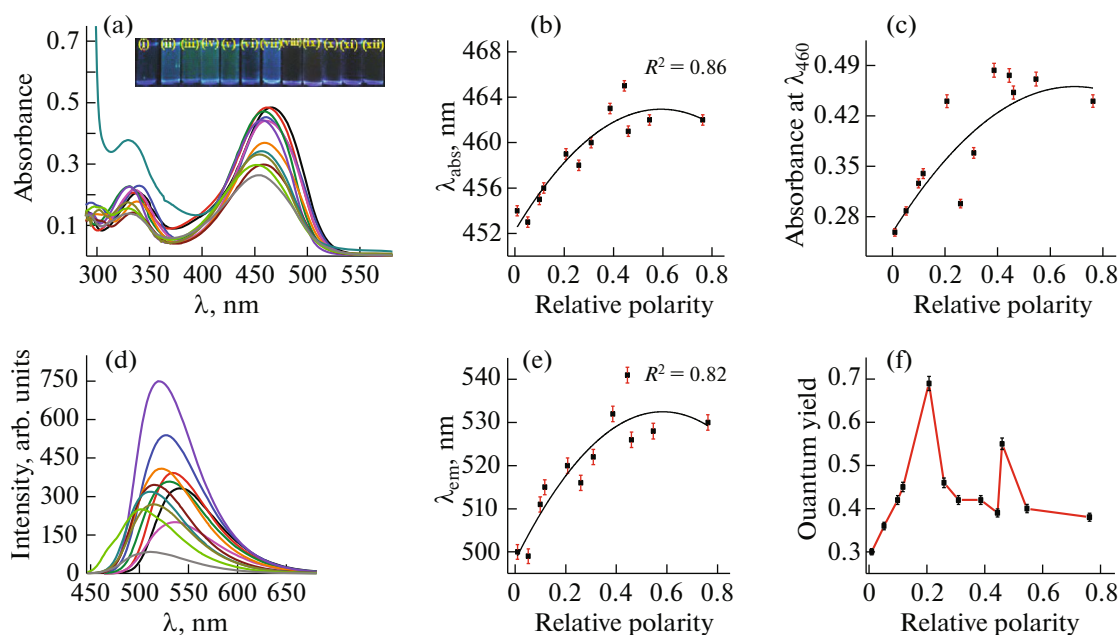
Fig. 1. Absorption (a) and fluorescence (d) spectral traces of **L** in different solvents, the plot of λ_{em} (b) and λ_{abs} (e) versus relative polarity of the solvents, the plot of absorbance at 460 nm (c) and quantum yield Φ (f) versus relative polarity of the solvents. The colour code of the solvents in plot (a, d): DMSO (black), DMF (red), CH_3CN (blue), CH_3OH (magenta), isopropanol (olive), DCM (orange), THF (violet), $CHCl_3$ (wine), diethylether (dark cyan), toulene (dark yellow), CCl_4 (green), hexane (grey).
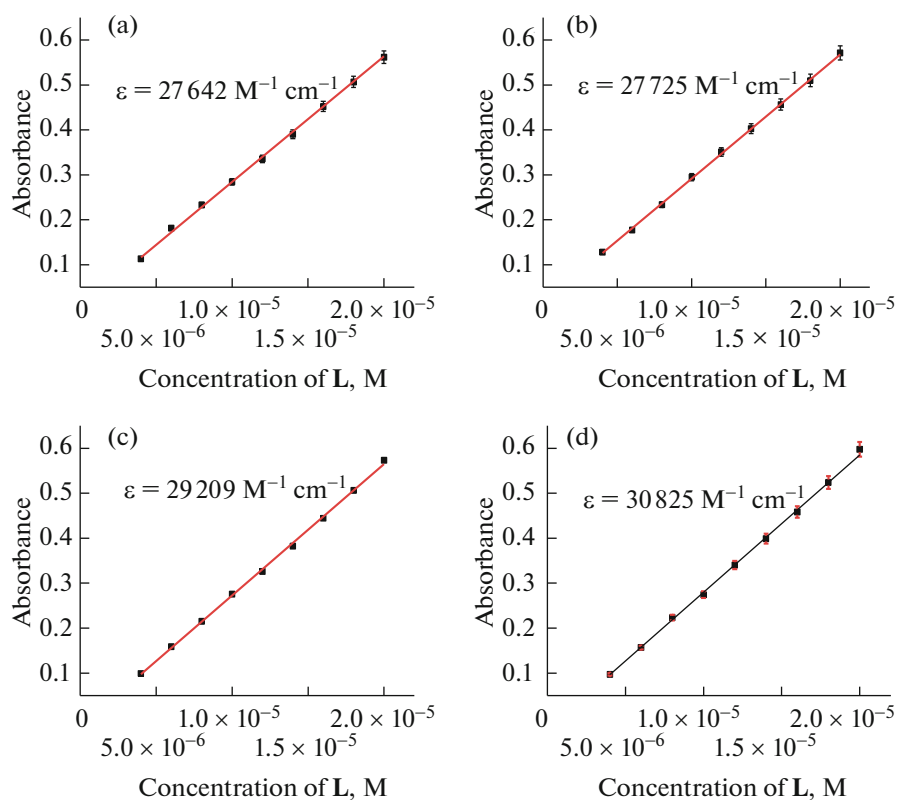
Fig. 2. Deriving molar extinction coefficient for **L** in different solvent: THF (a), DMSO (b), CCl_4 (c), methanol (d).
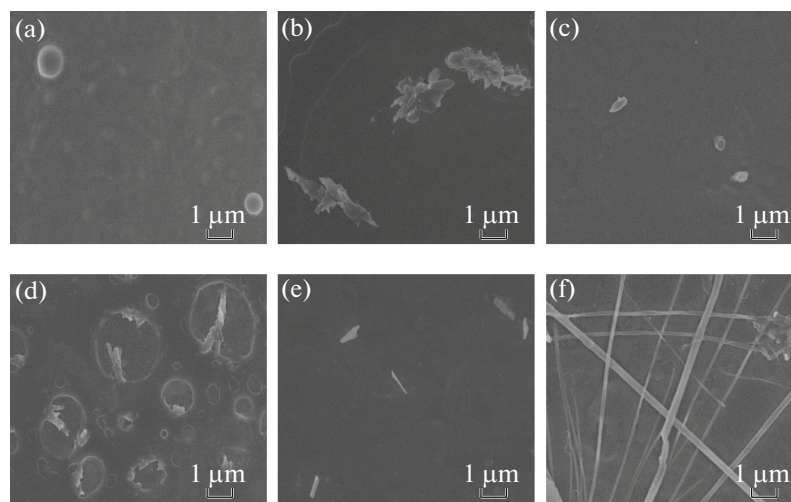
Fig. 3. SEM micrographs of the **L** in different solvents: $(CH_3)_2SO$ (a), CH_3CN (b), CH_3OH (c), C_4H_8O (d), CH_2CL_2 (e), CCl_4 (f).
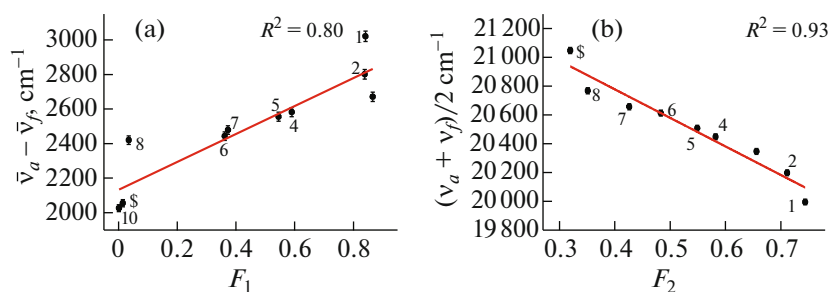
Fig. 4. The F_1 and F_2 are as given in Table 2. (a) Stokes' shift versus solvent polarity function F_1. (b) Arithmetic average of absorption and fluorescence wavenumbers versus solvent polarity function F_2. Solvents: DMSO (1), dimethylformamide (2), acetonitrile (3), dichloromethane (4), THF (5), chloroform (6), diethyl ether (7), toluene (8), carbontetrachloride (9), and *n*-hexane (10).

of the calix[4]arene are known to exhibit supramolecular aggregates. In polar protic solvent, such as CH_3OH, the **L** shows spherical structures and the morphology is distorted on going towards the aprotic polar solvent, such as $(CH_3)_2SO$, and the structures are far apart from each other in methanol. In THF, rod like morphology was obtained. In CH_3CN, these are more aggregated and stacked one over another with sharp edges protruding out. In CCl_4, nanowires (50–200 nm size) were obtained suggesting different aggregational behaviour for **L** when the solvent polarity is being changed.

Estimation of Ground and Excited State Dipole Moment for L

The effect of the polarity of the medium on the λ_{em}^{max} is more pronounced than that on the λ_{abs}^{max}. In order to get further information regarding the solvatochromic behaviour of **L**, the spectroscopic data are correlated with the relevant solvent polarity scales as shown in Figs. 4a, 4b and the trends are fairly linear. The linear behaviour of the solvent polarity versus Stokes' shift demonstrates the solvent effect as a function of refractive index and dielectric constant. The slopes of these linear plots yield $S_1 = 807.79$ cm^{-1} and $S_2 = 1395.04$ cm^{-1}, respectively. With the methodology and equations presented in the literature [22–24], the ground and excited state dipole moments of the molecule are estimated to be, $\mu_g = 2.1$ D and $\mu_e = 8.0$ D, respectively (Table 2). For this, an Onsager model radius (a_0) of 7.77 Å for the gas phase receptor

Table 2. Dipole moment of **L** in ground and excited states

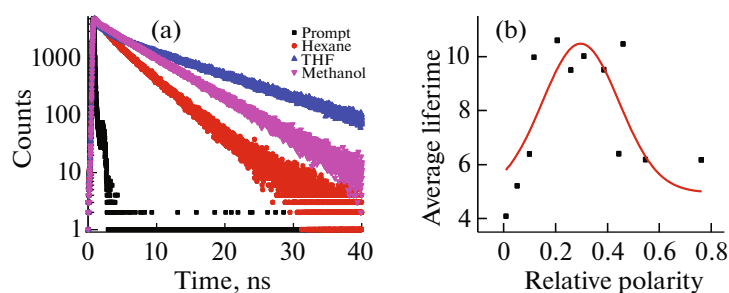| a_0, Å	S_1, cm^{-1}	S_2, cm^{-1}	μ_g, D	μ_e, D	$\Delta\mu$, D
7.77	807.79	1395.04	2.1	8.0	5.9

Fig. 5. (a) Fluorescence decay curves of compound in some selected solvents, (b) relative polarity versus average lifetime.

L was used as obtained from the computational studies (Onsager reaction field model at the aforementioned theory). All the data related to this study has been summarized in Table 3.

Thus the dipole moment is increased by four fold from the ground state of **L** to that in the excited state. This is attributable to the redistribution of the charge leading to charge transfer followed by bringing the conformational changes during the excitation. As the excited state exhibit greater dipole moment, it is more polar than that in the ground state of **L**. This is due to the specific solute−solvent interactions which are stronger in the excited state as compared to that in the ground state of **L**. All this is expected to bring red shift in the emission spectra and indeed the same is observed. Thus, an increase in the magnitude of the Stokes' shift was observed in polar solvents (3021.1 cm^{-1}) as compared to non polar solvents. The large change observed between the dipole moments of the ground and excited states is attributable to the presence of flexible arms on the lower rim of **L**.

Fluorescence Lifetime Measurements

The fluorescence lifetime decay of the receptor **L** was studied in different solvents at λ_{ex} = 440 nm by TCSPC as per the data given in Fig. 5a and Table 4. The fluorescence decay data were fitted well with bi-exponentials. From Fig. 5b, it is observed that the plot of average lifetime (τ) vs. relative polarity for receptor **L**, the data can be conveniently divided into three categories. In the range of 0 to 0.2, the τ increases rapidly w.r.t. the polarity and then remains unaltered in the range 0.2 to 0.4, however, decreases rapidly beyond 0.4. Thus, in polar protic solvent and non-polar solvents, the τ values are low as compared to polar aprotic solvents. The variance in the lifetime values is attributable to a different mode of hydrogen bonding interaction of **L** in different solvents in excited state. Specific interactions that are prevalent in protic solvents induce effective vibronic coupling with the excited state of **L** and thereby reducing the fluorescence quantum yield. Thus for the derivatives of calix[4]arene, there are large degrees of conformational flexibility, both in ground and excited state, to give a distribution of different structures with varying fluorescence decay times.

Table 3. Different solvent parameters and spectral data of **L**

Solvent	ε	η	F_1	F_2	$\overline{v_a} - \overline{v_f}$, cm^{-1}	$\dfrac{\overline{v_a} + \overline{v_f}}{2}$, cm^{-1}
DMSO	46.4	1.4770	0.8410	0.7440	3021.1	19994.8
DMF	38.0	1.4305	0.8387	0.7114	2801.3	20197.6
Acetonitrile	35.9	1.3442	0.8660	0.6560	2671.1	20346.9
DCM	8.9	1.4241	0.5900	0.5820	2582.0	20448.1
THF	7.6	1.4070	0.5450	0.5490	2555.7	20508.7
Chloroform	4.7	1.4459	0.3617	0.4831	2443.0	20612.6
DEE	4.3	1.3526	0.3730	0.4260	2478.8	20656.8
Toulene	2.3	1.4969	0.0330	0.3510	2420.1	20767.9
CCl$_4$	2.2	1.4610	0.0144	0.3193	2055.1	21047.6
n-Hexane	1.88	1.3749	0.0013	0.0024	2026.4	21013.2

Table 4. Fluorescence lifetimes of **L** in different solvents

Solvent	τ_1, ns	α_1	τ_2, ns	α_2	τ, ns	χ^2
DMSO	1.0	3.67	6.43	96.33	6.40	1.21
DMF	0.47	2.60	9.52	97.40	9.51	1.23
Acetonitrile	1.13	2.72	10.5	97.28	10.47	1.13
Methanol	0.23	1.32	6.18	98.68	6.17	1.22
Isopropanol	0.18	2.14	6.18	97.86	6.18	1.14
DCM	0.46	2.91	10.03	97.09	10.02	1.19
THF	1.13	7.79	10.68	92.31	10.60	1.21
Chloroform	0.55	3.26	9.52	96.74	9.50	1.19
DEE	0.86	6.17	10.03	93.83	9.97	1.21
Toulene	1.44	14.07	6.57	85.93	6.39	1.20
CCl$_4$	1.63	16.18	5.42	83.82	5.21	1.19
n-Hexane	1.43	13.13	4.22	86.87	4.08	1.17

CONCLUSIONS

Solvatochromic studies of a supramolecular and amphiphile, viz., benzofurazan appended calix[4]arene conjugate **L** has been carried out in 12 different solvents with varying polarity. The absorption and the emission spectral traces suggested the positive solvatochromism behaviour of **L** on going from nonpolar to polar solvents, i.e., ~10 and ~40 nm red shift in absorption and emission spectra, respectively. The ground state dipole moment value, μ_g estimated for **L** is 2.1 D and the excited state dipole moment is 8.0 D obtained from the solvatochromic shift method. The four fold increase in the dipole moment in the excited state of **L** is due to greater polar nature of the excited state. In the excited state it is likely that the charge separation increases, resulting in a large dipole moment than in the ground state. Aggregational behaviour of the **L** in presence of solvents of varying polarity revealed that aggregation or the receptor molecules is increased on going from the polar to non polar solvents.

REFERENCES

1. D. S. Chemla and J. Zyss, *Non-linear Optical Properties of Organic Molecules and Crystals* (Academic, New York, 1987).

2. W. Liptay and E. C. Lim, *Excited States* (Academic, New York, 1974), Vol. 1.

3. U. S. Raikar, C. G. Renuka, Y. F. Nadaf, B. G. Mulimani, A. M. Karguppikar, and M. K. Soudagarm, Spectrochim. Acta, Part A **65**, 673 (2006).

4. J. J. Aaron, M. D. Gaye, C. Parkanyi, N. S. Cho, and L. von Szentpaly, J. Mol. Struct. **156**, 119 (1987).

5. J. J. Aaron, A. Times, M. D. Gaye, C. Parkanyi, C. Boniface, and T. W. N. Biezev, Spectrochim. Acta, Part A **47**, 419 (1991).

6. C. Parkanyi, S. R. Oruganti, A. O. Abdelhamid, L. V. Szentpaly, B. Ngom, and J. J. Aaron, J. Mol. Struct.: THEOCHEM **135**, 105 (1986).

7. R. Giri and M. M. Bajaj, Curr. Sci. **62**, 522 (1992).

8. J. Czekella, Zeitschr. Chem. **15**, 26 (1961).

9. S. Joshi and D. D. Pant, J. Mol. Liq. **166**, 49 (2012).

10. S. Joshi and D. D. Pant, J. Mol. Liq. **172**, 125 (2012).

11. Z. Ma, Y. Lin, H. Chen, L. Du, and M. Li, RSC Adv. **6**, 102773 (2016).

12. M. Amaro, H. A. L. Filipe, J. P. P. Ramalho, M. Hof, and L. M. S. Loura, Phys. Chem. Chem. Phys. **18**, 7042 (2016).

13. Y. L. Pak, K. M. K. Swamy, and J. Yoon, Sensors **15**, 24374 (2015).

14. X.-J. Cao, L.-N. Chen, X. Zhang, J.-T. Liu, M.-Y. Chen, Q.-R. Wu, J.-Y. Miao, and B.-X. Zhao, Anal. Chim. Acta **920**, 86 (2016).

15. F. Zhang, Y. Sun, D. Tian, W. S. Shin, J. S. Kim, and H. Li, Chem. Commun. **52**, 12685 (2016).

16. S. B. Nimsea and T. Kim, Chem. Soc. Rev. **42**, 366 (2013).

17. A. Nehra, V. K. Hinge, and C. P. Rao, J. Org. Chem. **79**, 5763 (2014).

18. M. Deska, B. Dondela, and W. Sliwa, ARKIVOC, No. VI, 393 (2015).

19. R. Joseph and C. P. Rao, Chem. Rev. **111**, 4658 (2011).

20. V. V. S. Mummidivarapu, A. Nehra, V. K. Hinge, and C. P. Rao, Org. Lett. **14**, 2968 (2012).

21. A. Nehra, S. Bandaru, D. S. Yarramala, and C. P. Rao, Chem. Eur. J. **22**, 8903 (2016).

22. N. G. Bakhshiev, Opt. Spektrosk. **16**, 821 (1964).

23. L. Bilot and A. Kawski, Zeitschr. Naturforsch. **17a**, 621 (1962).

24. L. Bilot and A. Kawski, Zeitschr. Naturforsch. **18a**, 256 (1963).

25. J. Olmsted, J. Phys. Chem. **20**, 2581 (1979).

26. C. Ranjitha, K. K. Vijayana, V. K. Praveena, and N. S. Saleesh, Spectrochim. Acta, Part A **75**, 610 (2010).

27. B. Uttam, R. Kandi, M. A. Hussain, and C. P. Rao, J. Org. Chem. **83**, 11850 (2018).